analytical chemistry

pubs.acs.org/ac Article

Size Exclusion Chromatography: An Indispensable Tool for the Isolation of Monodisperse Gold Nanomolecules

Naga Arjun Sakthivel,[†] Vijay Reddy Jupally,[†] Senthil Kumar Eswaramoorthy, Kalpani Hirunika Wijesinghe, Praneeth Reddy Nimmala, Chanaka Kumara, Milan Rambukwella, Tanya Jones, and Amala Dass*

Cite This: *Anal. Chem.* 2021, 93, 3987−3996 Read Online

ACCESS | Metrics & More | Article Recommendations | Supporting Information

ABSTRACT: Highly monodisperse and pure samples of atomically precise gold nanomolecules (AuNMs) are essential to understand their properties and to develop applications using them. Unfortunately, the synthetic protocols that yield a single-sized nanomolecule in a single-step reaction are unavailable. Instead, we observe a polydisperse product with a mixture of core sizes. This product requires post-synthetic reactions and separation techniques to isolate pure nanomolecules. Solvent fractionation based on the varying solubility of different sizes serves well to a certain extent in isolating pure compounds. It becomes tedious and offers less control while separating AuNMs that are very similar in size. Here, we report the versatile and the indispensable nature of using size exclusion chromatography (SEC) as a tool for separating nanomolecules and nanoparticles. We have demonstrated the following: (1) the *ease of separation* offered by SEC over solvent fractionation; (2) the separation of a *wider size range* (∼5−200 kDa or ∼1−3 nm) and *larger-scale* separation (20−100 mg per load); (3) the separation of *closely sized AuNMs*, demonstrated by purifying $Au_{137}(SR)_{56}$ from a mixture of $Au_{329}(SR)_{84}$, $Au_{144}(SR)_{60}$, $Au_{137}(SR)_{56}$, and $Au_{130}(SR)_{50}$, which could not be achieved using solvent fractionation; (4) the separation of *AuNMs protected by different thiolate ligands* (aliphatic, aromatic, and bulky); and (5) the separation can be improved by increasing the column length. Mass spectrometry was used for analyzing the SEC fractions.

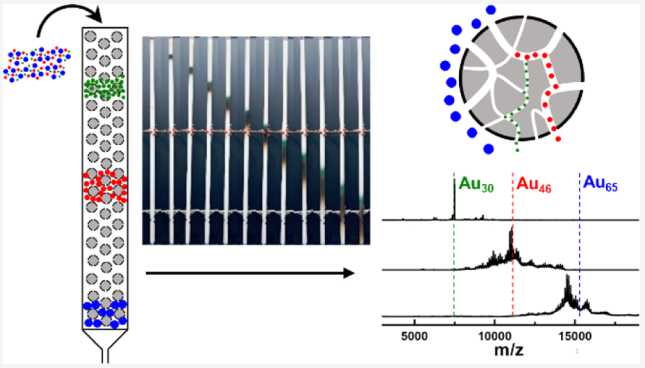

INTRODUCTION

Gold nanomolecules (AuNMs) (also known as nanocrystals and nanoclusters) are atomically precise ultrasmall thiolate protected gold nanoparticles.[1−5] The AuNM preparation involves a two-step protocol. The first step involves preparation of a crude product following a two-phase (Brust−Schiffrin) method[6] or a single-phase method [using tetrahydrofuran (THF) as the solvent]. The crude product is polydisperse in nature, consisting of a mixture of sizes. The second step involves thermochemical treatment of the product at an elevated temperature in the presence of an excess amount of the ligand. The thermochemical treatment is also referred to etching.[7] The etching step results in a product with narrowed size distribution, where the products are atomically precise and thermodynamically stable. The availability of such precise compounds[8] has enabled us to understand the structure and property evolution in the ultrasmall size range of 1−3 nm.[9] The research interest on AuNMs is growing exponentially due to their high stability[8] and unique optical[10−12] and electronic properties[3,10,13−19] with potential applications in biomedicine, catalysis, etc.[20−22]

Exploring the fundamental properties and practical applications of AuNMs requires monodisperse products. Therefore, the use of separation techniques becomes unavoidable. Separation techniques such as solvent fractionation,[8,23] high-pressure liquid chromatography (HPLC),[24−30] size exclusion chromatography (SEC),[31−36] and preparative thin-layer chromatography (PTLC)[37] have been widely employed in isolating pure AuNMs. Whetten et al. employed solvent fractionation for isolating organosoluble AuNMs in their seminal work.[1] Solubility of the AuNMs varies with the size. In organosoluble AuNMs, smaller sizes are soluble in polar solvents like acetonitrile and acetone, while larger sizes are soluble in solvents like toluene, dichloromethane (DCM), and THF. The difference in the solubility of AuNMs is exploited in solvent fractionation. As the polarity of the solution increases,

Received: November 25, 2020
Accepted: February 8, 2021
Published: February 19, 2021

Table 1. SEC Column Parameters[a]

	Long	Medium	Short
Column length (cm)	199.4	149.9	60.9
Expanded bed Length (cm)	196.8	138.4	54.6
Bed length (cm)	180.3	130.8	50.8
Inner diameter (cm)	2.64	2.64	2
Outer diameter (cm)	3.2	3.2	2.54
Tip OD (cm)	1.04	1	1
Tip Length (cm)	~5	~5	~6.4
Frit to tip length (cm)	~11.4	~11.4	~11.4
Flow Rate (ml/min)	0.65	1.05	1.3
Optimum loading mass (mg)	50-100	35-40	15-20
Elution time (hours)	~16-18	~4-6	~1-1.5
Beads	Bio-Rad SX-1 Support		

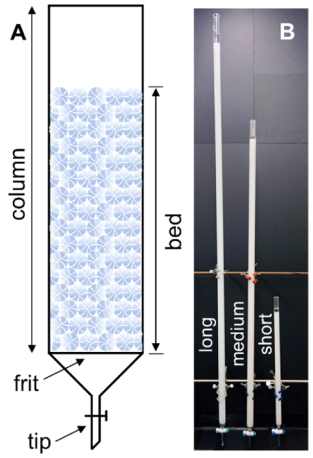

[a]The column dimensions are shown in (A), and three column images are shown in (B).

the larger sizes precipitate first, followed by the smaller sizes. This technique gives minimal control and is a tedious process, but it can be used reproducibly with practice. HPLC of organosoluble thiolate-capped AuNMs has been explored widely.[24−30] The separation takes place based on varying intermolecular interactions between the analyte and the stationary phase. It offers a quantitative insight into the polydisperse nature (distribution of various sizes) of the sample. The electrochemical, UV−visible, and mass spectrometric detection of various fractions has been employed, enabling their identification and characterization.[24−29] However, to enable further detailed studies, it is challenging to process tens of milligrams of the product using HPLC. The PTLC[37] technique has also been used to isolate AuNMs. In the case of PTLC, a significant amount of human interaction is involved with spotting the sample, plate development, and then recovering each separated species from the plate (by scrapping and further processing). In some cases, column chromatography (CC) has also been employed (using alumina or silica beads) in the separation of AuNMs.[18,38] Gel electrophoresis (and various chromatographic methods) has also been used in the case of water-soluble thiolate ligand-protected (Au and Ag) nanomolecules.[39−42] We also refer the reader to a review article by Negishi et al.; it comprehensively details various types of separation techniques being used in the separation of nanomolecules.[41]

SEC was originally developed for separation of proteins, lipids, fatty acids, lipophilic polymers, and polycyclic aromatic compounds.[43−45] The separation by SEC is based on the hydrodynamic volume (size) of the nanomolecules.[34] The smaller-sized compounds travel through the pores in the beads and take a longer path to elute. The larger sizes take a shorter path and elute faster through the larger pores or spaces between the beads. Thus, the larger nanomolecules elute first and the smaller nanomolecules elute later. SEC is straightforward and offers better control than solvent fractionation. In the literature, the majority of the work employing SEC for separation of nanomolecules (or nanoparticles) has used HPLC instruments with a commercial SEC column and different types of detectors.[31−33,35] The use of sophisticated instruments severely limits the quantity of the product that can be separated per run. Knoppe et al. performed semi-preparative-scale SEC to separate $Au_{38}(SR)_{24}$ and $Au_{40}(SR)_{24}$ using a gravity flow CC-type setup.[34] It enabled loading ~40 mg of the product per run for separation. The styrene divinylbenzene-based Bio-Beads S-X1 support was used as the stationary phase in a glass column (typically used for CC), and THF (stabilized with butylated hydroxytoluene, THF-BHT) was used as the mobile phase.

Here, we demonstrate the versatility and the indispensable nature of the gravity flow SEC technique to isolate the organosoluble thiolate ligand-capped AuNMs. We have elucidated the following: (1) the *control and ease* of separation offered by SEC compared to solvent fractionation, (2) separation of *a wide range of sizes* (a crude nanoparticle mixture ranging from ~5 to ~200 kDa), (3) separation of *closely sized AuNMs* [$Au_{137}(SR)_{56}$ from a mixture of $Au_{329}(SR)_{84}$, $Au_{144}(SR)_{60}$, $Au_{137}(SR)_{56}$, and $Au_{130}(SR)_{50}$], (4) separation of *AuNMs protected by different ligands* (phenylethanethiolate, thiophenolate, 4-*tert*-butylbenzene thiolate, and *tert*-butyl thiolate), and (5) separation (resolution) can be improved by increasing the column length. Matrix-assisted laser desorption ionization mass spectrometry (MALDI-MS) has been primarily used for the analysis of fractions collected from SEC. Electrospray ionization (ESI) MS was utilized for the analysis of fractions from the separation of closely sized AuNMs. MALDI-MS analysis of samples is recommended as it provides a better representation of the sample content. However, ESI-MS serves primarily as an identification technique to assign precise composition. ESI-MS could be misleading sometimes as one AuNM would be relatively easy to ionize and that AuNM may not be the major component in the sample. The soft-ionization technique of ESI-MS coupled with higher mass resolution enables identification of larger nanomolecules and closely related sizes.

We have used glass columns of three different lengths with fritted discs for the gravity flow SEC (Table 1), the Bio-Beads S-X1 support as the stationary phase, and THF-BHT as the mobile phase. The Bio-Beads is made of neutral, porous styrene divinylbenzene copolymers that are soaked in organic solvents and packed in a glass column.[45] The extent of cross-linking determines the pore size of the beads. Solvents such as benzene, DCM, carbon tetrachloride, perchloroethylene, dimethylformamide, and trichlorobenzene can also be used, and the choice of the solvent affects the pore size of the beads.[45] The size exclusion range specified by the manufacturer

https://dx.doi.org/10.1021/acs.analchem.0c04961
Anal. Chem. 2021, 93, 3987−3996

for these beads is from 600 to 14,000 Da. However, these beads have proven to separate nanoparticles as large as 200 kDa. The gravity flow SEC columns can be set up under a fume hood with no special controls. The size of the column can be tailored to requirement. However, HPLC requires a sophisticated setup and optimization of the type and size of the separation column. The ease of operation coupled with the control over the separation of closely related sizes makes SEC a powerful indispensable tool to isolate monodisperse nanomolecules in a preparative scale. Our group has used these setups for almost a decade and published reports on numerous AuNMs and their properties and applications (we refer the reader to some of our reports using SEC[9,36,46−49]).

EXPERIMENTAL SECTION

Materials. Hydrogen tetrachloroaurate(III) ($HAuCl_4 \cdot 3H_2O$) (Alfa Aesar, ACS grade), tetraoctylammonium bromide (Sigma-Aldrich, 98%), sodium borohydride (Acros, 99%), thiophenol (Acros, 99%), phenylethyl mercaptan (Sigma-Aldrich, ≥99%), 4-*tert*-butylbenzenethiol (TBBTH) (TCI Chemicals, >97%), *tert*-butylthiol (Sigma-Aldrich, 99%), cesium acetate (Acros, 99%), anhydrous ethyl alcohol (Acros, 99.5%), and *trans*-2-[3[(4-tertbutylphenyl)-2-methyl-2-propenylidene] malononitrile (DCTB matrix) (Fluka ≥99%) were used as received. HPLC-grade solvents such as THF, toluene, methanol, THF-BHT, and acetonitrile were obtained from Fisher Scientific. The Bio-Beads S-X1 support resin (styrene divinylbenzene beads; mesh size, 200−400; cross-linkage, 1%; bead size, 40−80 μm; exclusion range, 600−14,000 Da) was obtained from Bio-Rad Laboratories.

Synthesis. The samples utilized to demonstrate the use of SEC for nanomolecules were prepared following the reported protocols. We refer the reader to the corresponding references for the synthetic procedures: Au_{67} and $Au_{\sim 103-105}$ (refs 23 and 50), $Au_{137}(SR)_{56}$ (ref 36), thiophenolate-protected AuNMs (refs 51 and 52, TBBT-protected $Au_{28}(SR)_{20}$, $Au_{36}(SR)_{24}$, and $Au_{44}(SR)_{28}$ (ref 53), and *t*-butylthiolate-protected AuNMs (ref 49).

Instrumentation. A Voyager DE Pro mass spectrometer operated with a N_2 laser at 337 nm in the positive mode was used to obtain the MALDI-MS data. About 2 μL of the eluted SEC fraction (without rotary evaporation and washing) was mixed with 1 μL of the freshly prepared DCTB[54] matrix (100 mg/mL toluene) in an Eppendorf tube (0.5 mL) and spotted on a well in the MALDI target plate. Compositional analysis was performed by ESI-MS. ESI-MS were recorded using a Waters Synapt HDMS instrument. The eluted fractions were rotary-evaporated to dryness and washed with methanol (couple of times). Then, the ESI-MS sample was prepared by dissolving the sample in THF, where the concentration is ∼0.5−1 mg/mL. The sample solution was mixed with cesium acetate to facilitate the ionization of (neutral) AuNMs via cesium adduct formation. Typically, cesium acetate (20 μL, 50 mg/mL) was added to the sample (150 μL) and mixed prior to introducing the sample via the ESI source.

Solvent Fractionation. A polydisperse product was dissolved in an organic solvent such as toluene, DCM, or THF. The polarity of the solution was gradually increased by the addition of methanol or acetonitrile. An optimum concentration of the polydisperse mixture was used to achieve better separation. A highly concentrated solution would lead to poor separation, whereas dilute solutions would require large volumes of acetonitrile or methanol. Typically, 100 mg of a polydisperse product was dissolved in 0.2−1 mL of the solvent. The non-solvent was then gradually added using a micropipette in small quantities (typically in multiples of 100 μL). Once the precipitate was observed, the vial was centrifuged to separate the precipitate (insoluble portion) from the supernatant (soluble portion). The fractions were then analyzed by MS to determine their composition.

Size Exclusion Chromatography. Columns of three different lengths were used in the present work. They are named short (∼61 cm), medium (∼150 cm), and long (∼200 cm) based on their length (Table 1). About 100 g of the solid beads was soaked in ∼0.5 L THF-BHT in a 1 L beaker topped with a lid to prevent solvent evaporation. The beads were soaked for at least 6 h, preferably overnight. The beads expand in volume during this time. The choice of the solvent was THF-BHT as it is compatible with the beads and dissolves the nanomolecules of a wide size distribution. After sufficient soaking, the slurry of swollen beads was then packed in the column. The columns for SEC were ordered from Chemglass with the dimensions listed in Table 1, a Teflon stopcock, a coarse fritted disc, and a beaded top. The slurry was slowly loaded through the side of the column with the stopcock open and the excess solvent to avoid any air bubbles. The excess THF elutes out as the beads settle and pack in the column. The column was packed with beads until the final level of the bed was ∼4 inches from the top. Once the beads were completely packed, the stopcock was closed. It is important to make sure that the column never runs out of the solvent to avoid drying of the beads.

Sample Preparation. The polydisperse product to be separated was dissolved in THF-BHT and centrifuged at 1252 times of gravity (4000 rpm for 3−4 min) to precipitate any insoluble material. The supernatant was separated, dried, and weighed for loading on the SEC columns. Based on the column size used for separation, varying amounts of the crude product were loaded on the SEC columns (Table 1). The product was dissolved in a minimal amount of the solvent (∼0.1−0.2 mg/μL) for better separation.

Loading. The SEC bed expands in volume when it is idle. Therefore, the solvent above the bed level was eluted until the bed reached a constant height. The bed surface was made flat by stirring it with a glass rod/pipette during this process. After the settled bed was flat and constant in height, the solvent above the bed was eluted to the level of the bed. The stopcock was closed soon after the flat white surface of the bed was visible (elution of the excess solvent would make the beads dry and result in air bubbles affecting the separation). The dissolved sample was taken in a 9″ Pasteur pipette and loaded carefully (drop by drop), spreading it across the surface as a thin disk (layer). The loading step is crucial for better separation. The stopcock was opened and after 5−10 s, the fresh mobile phase was added to allow the loaded the sample to enter the bed. The solvent was added evenly on the surface of the thin band drop by drop using a Pasteur pipette in circular motion. The shape of the band was maintained flat by adding the solvent uniformly. The solvent was added in a similar fashion until the band was ∼3 cm below the surface of the bed, and the solvent level was ∼3 cm above the surface of the bed. The solvent was then added along the walls of the column using a Pasteur pipette to minimize disturbing the surface of the SEC bed. The solvent can then be added directly from the solvent wash bottles along the walls. The solvent level was maintained by refilling during the elution process. The

https://dx.doi.org/10.1021/acs.analchem.0c04961
Anal. Chem. 2021, 93, 3987−3996

overloading of the product would cause bleeding and reduces the separation. The uneven loading would lead more nanoparticles to be accumulated on one side of the column and eventually result in mixing of different sizes. It would appear as streaks on one side. The loading skill can be honed by practicing it a few times. An example for a typical SEC sample loading is illustrated in Figure S1.

Elution and Elution Time. During the elution, no solvent was allowed to be trapped in the space between the glass frit and stopcock. The solvent trapped between the glass frit and stopcock mixes the eluting product and adversely affects the separation. Elution time varies significantly based on the size of the AuNM and the column dimension. Elution times listed in Table 1 were the representative times recorded from elution of various products (different size ranges, ligands, and compositions). The stopcock was closed after all the product was eluted. Fractions collected from SEC were then analyzed by MS to determine the composition. The fractions are washed with excess methanol after rotary evaporation to remove the residual BHT for storage or crystallization setups of the desired product.

Maintenance. When the SEC bed dried out, the beads were transferred into a beaker by passing a low-pressure stream of air through the stopcock. The beads were soaked in THF-BHT for ∼12 h, stirred intermittently with a glass rod, and reused. Beads gradually deteriorate over time, and measuring the flow rate quarterly acts as a good indicator of the performance of the column. A significant increase in flow rate over time indicates a higher chance of channeling (band broadening due to rapid flow of the solvent and analyte compared to usual) to occur.

RESULTS AND DISCUSSION

SEC gives access to highly pure samples for characterization and other applications. SEC of different types of nanomolecule mixtures was performed to demonstrate the versatility of the technique. Here, we discuss the effectiveness of SEC in comparison to solvent fractionation, the separation range, separation of closely related sizes, AuNMs protected by different ligands, and the effect of the column length on separation. Fraction numbers are denoted as F1, F2, etc., and soluble/insoluble are shortened as sol/insol for clarity. The first fraction eluting from the column was labeled as F1, and subsequent fractions were labeled with increasing numbers.

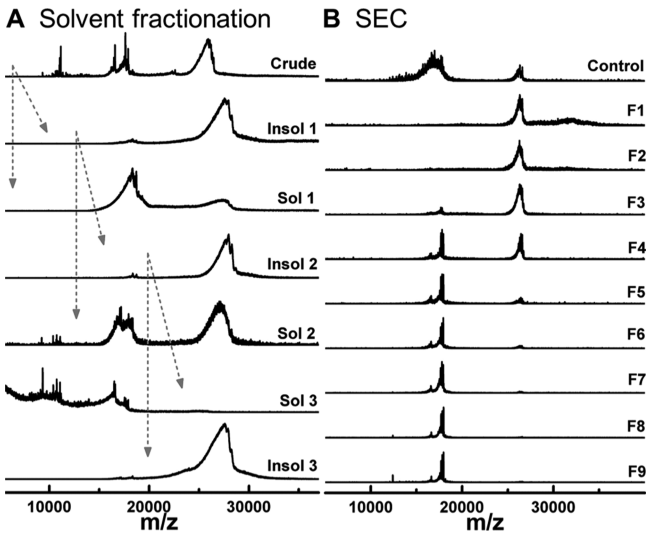

Figure 1. SEC vs solvent fractionation. MALDI-MS of the fractions from the (A) solvent fractionation and (B) SEC to separate $Au_{\sim 103-105}$ and Au_{67} nanomolecules using a small column.

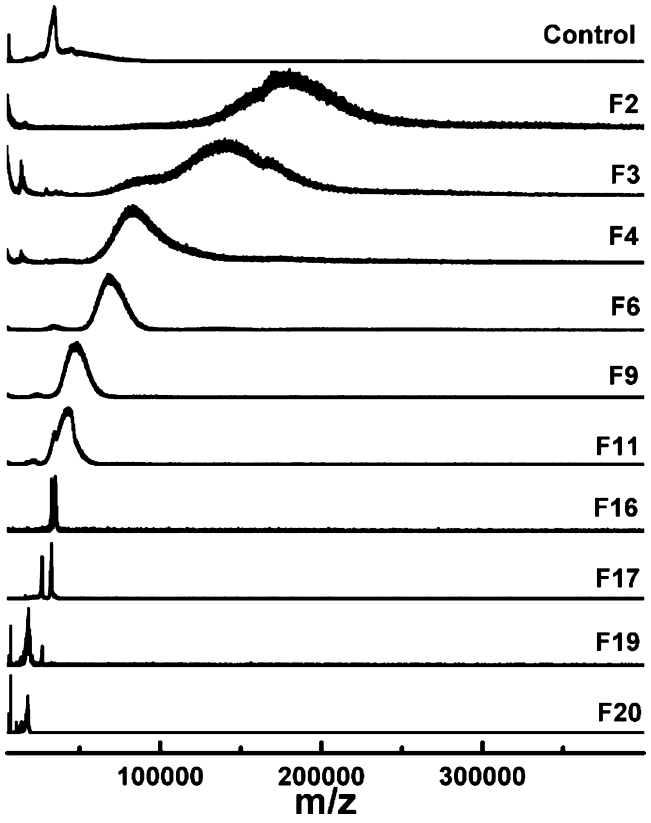

Figure 2. SEC of a polydisperse sample with m/z ranging from ∼5 to 200 kDa. Positive mode MALDI-MS of several fractions collected from the long column is reported (and a few identical fractions are excluded for clarity).

Solvent Fractionation versus SEC. Solvent fractionation is a very tedious and time-consuming process with minimal control compared to SEC. To demonstrate the effectiveness of the SEC technique, both SEC and solvent fractionation were employed to separate a mixture of Au_{67} and $Au_{\sim 103-105}$ nanomolecules.[23,50]

The fractions obtained from both the techniques were analyzed using MALDI-MS (Figure 1). Figure 1A reveals the solvent fractionation of a mixture of $Au_{\sim 103-105}$ and Au_{67}. The gray arrows indicate the source of samples for different fractionation steps during the three cycles. First, the crude product was dissolved in toluene and precipitated with methanol. The soluble and insoluble fractions were separated and labeled as Sol 1 and Insol 1, respectively. Insol 1 comprised a major amount of $Au_{\sim 103-105}$ and minor amounts of Au_{67}. It was further fractionated using toluene and methanol to obtain Insol 2 and Sol 2. $Au_{\sim 103-105}$ was the most dominant species in Insol 2, and it was further fractionated. The soluble and insoluble fractions obtained from Insol 2 were labeled as Insol 3 and Sol 3. Insol 3 showed nearly pure $Au_{\sim 103-105}$ mass spectra. The separation of $Au_{\sim 103-105}$ by solvent fractionation took three cycles; some of $Au_{\sim 103-105}$ was lost in fractions Sol 1 and Sol 2, and the separation was not perfect.

SEC separation of a mixture of $Au_{\sim 103-105}$ and Au_{67} nanomolecules in one cycle is shown in Figure 1B. In SEC,

https://dx.doi.org/10.1021/acs.analchem.0c04961
Anal. Chem. 2021, 93, 3987−3996

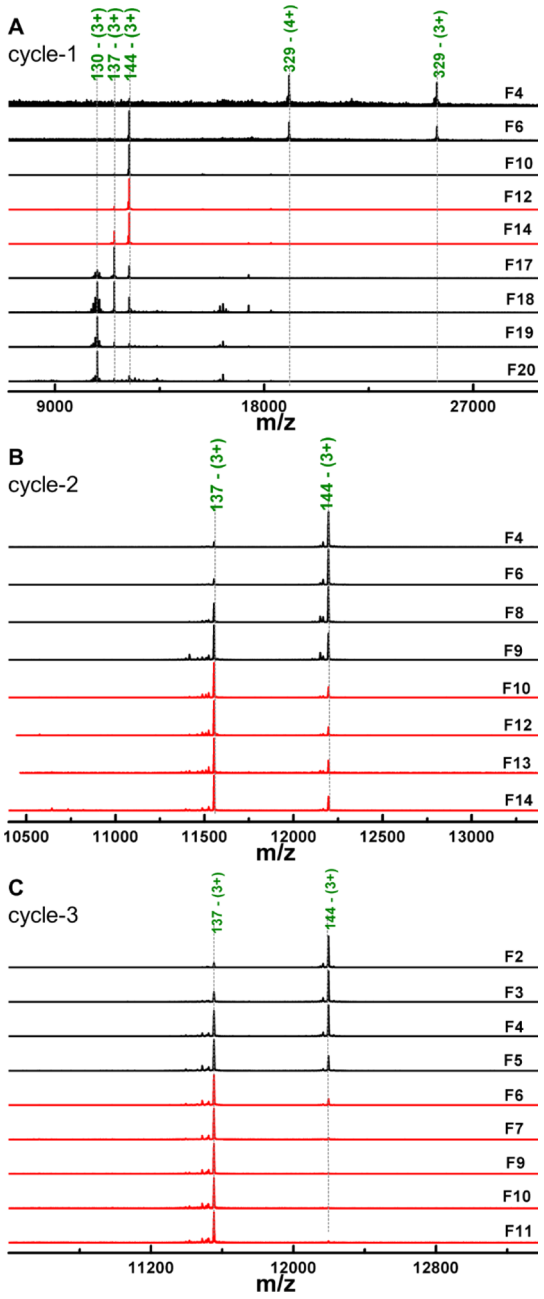

Figure 3. Purification of $Au_{137}(SR)_{56}$ from a mixture of closely related sizes using SEC. ESI-MS of (A) the fractions collected from SEC of the starting material. Fractions F12 through F14 (in red) were used for the (B) second SEC cycle. Fractions F10 through F14 from the second SEC cycle were used as the starting material for the (C) third SEC cycle, where pure $Au_{137}(SR)_{56}$ was obtained.

larger sizes elute first, followed by smaller sizes. $Au_{\sim 103-105}$ was predominant in fractions F2 and F3. Note that better separation could be achieved by collecting more fractions from the column. Pure Au_{67} was obtained in fractions F8 and F9. There was minimal loss of the desired product in the form of mixtures as compared to solvent fractionation. The mixtures can further be separated using multiple SEC cycles. On the other hand, solvent fractionation did not yield the pure product even after multiple fractionation steps. The separation observed in both the techniques readily demonstrates the superior performance of SEC in separating AuNMs in terms of both the effective separation and the processing time.

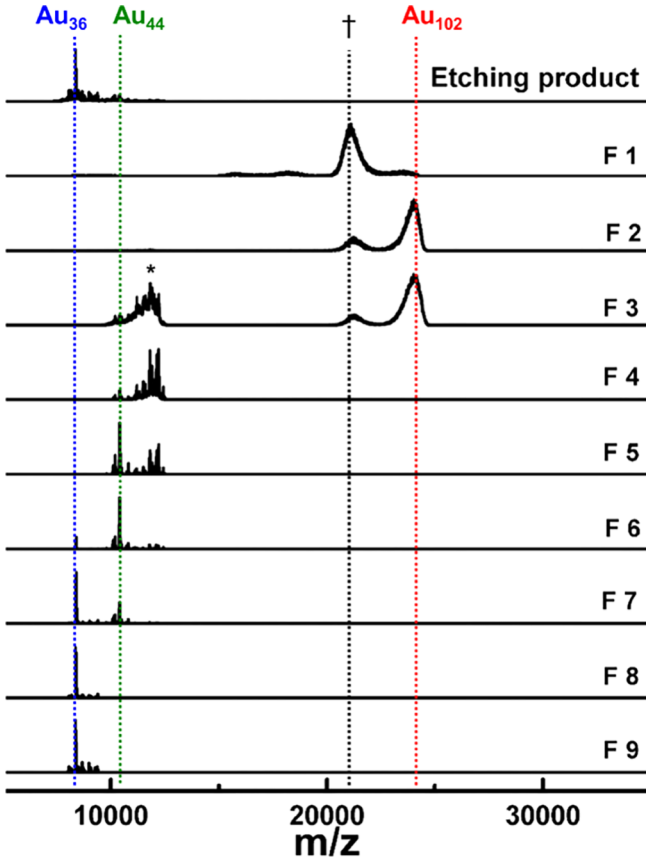

Figure 4. SEC of a thiophenolate-protected AuNM sample. Positive mode MALDI-MS of the fractions collected from short column separation of $Au_{36}(SPh)_{24}$ from Au_{44} and Au_{102} in the sample. † indicates the Au_{102} core, and * indicates the unidentified AuNM species.

SEC Separation of a Wide Range of AuNM Sizes. The manufacturer specification for Bio-Beads S-X1 in separation of proteins and polymers is from 600 to 14,000 Da. This mass range might not apply to AuNMs. To investigate the size exclusion range for AuNMs, a crude product with sizes ranging from ∼5 to ∼200 kDa was used for SEC separation.

Figure 2 reports the MALDI-MS data for different fractions collected from SEC of the polydisperse crude product. The crude product has a major peak of ∼35 kDa, but there were also larger clusters in the sample. They were obscured due to the ease of ionization of smaller sizes compared to larger sizes. It led to the high intensity peak for the smaller sizes. A total of 20 fractions were collected from this separation. The fractions showing similar nanomolecule distributions were omitted for clarity. Since larger sizes elute before smaller sizes, the first three fractions had sizes ranging from 100 to 200 kDa. Later fractions showed sizes ranging from 10 to 100 kDa. This separation proves that AuNMs as large as 200 kDa can be separated using SEC. Also, the total exclusion limit (where the sizes beyond a certain limit do not undergo any separation) is not reached at 200 kDa for AuNMs. The crude product used for separation was not etched. Therefore, nanoclusters with broad peaks were observed in the MALDI mass spectra of fractions F2−F9. A majority of AuNMs reported to date are in the mass range of 5−250 kDa, and SEC using Bio-Beads S-X1 would be suitable to isolate them in a semi-preparative or preparative scale.

https://dx.doi.org/10.1021/acs.analchem.0c04961
Anal. Chem. 2021, 93, 3987−3996

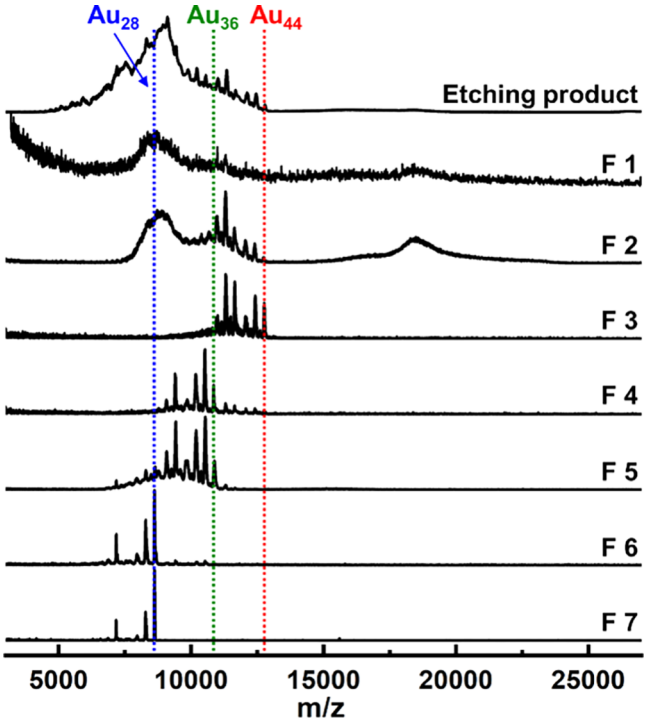

Figure 5. SEC of a TBBT-protected AuNM etch product consisting of periodic compounds with a difference of $Au_8(TBBT)_4$. MALDI-MS of the fractions collected from the short column separation of $Au_{28}(TBBT)_{20}$, $Au_{36}(TBBT)_{24}$, and $Au_{44}(TBBT)_{28}$ is shown. The vertical dotted lines correspond to the one ligand loss peak of each species. Lines are provided to readily identify each species and their fragment peaks to the left of the parent ion peak.

SEC of Closely Related AuNM Sizes. AuNMs of various sizes are observed during the crude synthesis and etching reactions. Some of these sizes only vary by few atoms. SEC of such closely related sizes is difficult, and several cycles are required. Knoppe et al. reported the separation of Au_{38} and Au_{40} nanomolecules by multiple SEC separation cycles.[34] When two closely related sizes are passed through SEC, the fractions collected are dominated by one of the species. Separation of three closely related sizes becomes increasingly difficult because of the similarity in their size. Our group reported the isolation of $Au_{137}(SR)_{56}$ from a polydisperse mixture by performing multiple SEC cycles, which could not be achieved by solvent fractionation.[36]

In this experiment, $Au_{137}(SR)_{56}$ was separated from a mixture of $Au_{130}(SR)_{50}$, $Au_{137}(SR)_{56}$, and $Au_{144}(SR)_{60}$. The three sizes only vary by few gold atoms and ligands, making the separation difficult, that is, although they vary in molecular weight, they are comparable in size. Also, the peaks for these three nanomolecules cannot be distinguished in MALDI-MS, so the separation needs to be monitored by ESI-MS. The separation was achieved by three SEC cycles (Figure 3). The starting material contained a mixture of $Au_{329}(SR)_{84}$, $Au_{144}(SR)_{60}$, $Au_{137}(SR)_{56}$, and $Au_{130}(SR)_{50}$ (−SR corresponds to phenylethanethiolate). The MALDI-MS spectra of the starting material are shown in Figure S2, and other smaller (<30 kDa) and larger (>80 kDa) sizes were also present in the sample (Figure S3). SEC fractions were monitored by ESI-MS, which shows multiply charged peaks. Table S1 details the mass/charge (m/z) values of these nanomolecules at different charge states. Mass spectra in red were used to indicate fractions with Au_{137} as the major species (Figure 3).

Figure 3 shows the fractions collected from SEC. Redundant fractions with similar size distribution are not shown here for clarity. In the first cycle (Figure 3A), $Au_{329}(SR)_{84}$ eluted first and was dominant in fractions F4 through F6. Fractions F10−F12 had pure $Au_{144}(SR)_{60}$. Fractions F13 and F14 had a mixture of $Au_{144}(SR)_{60}$ and $Au_{137}(SR)_{56}$. Fractions F17−F19 contained a mixture of Au_{144}, Au_{137}, and Au_{130} (their 3+ charge state peaks are indicated in the figure and the 2+ charge state peaks can be found in the 16−18.5 kDa range, see Table S1). Fraction F20 contained pure Au_{130}. Fractions with pure Au_{137} were not obtained from this separation. For further purification, samples with Au_{144} and Au_{137} were combined for another cycle of SEC. Fractions with Au_{130} were avoided as its separation would be difficult. Fractions F12 through F14 from the first SEC cycle were combined and used for the next cycle.

Figure 3B shows the fractions obtained from the second cycle. Fractions F1−F3 did not show any peaks in ESI-MS. Au_{144} was dominant in fractions F4−F8, and Au_{137} was dominant in fractions F10−F14. The second cycle did not yield pure Au_{137}. Fractions F10−F14 were combined for a third SEC cycle.

Figure 3C shows ESI-MS of the fractions collected from the third SEC. Pure Au_{137} was isolated in fractions F6 through F11. Pure $Au_{137}(SR)_{56}$ was characterized by various analytical techniques, and catalytic properties were investigated.[36] SEC can be used to separate very closely related sizes as demonstrated in this experiment. Notably, these three closely related sizes were also identified in a commercially available 2 nm gold nanoparticle product.[27]

Separation of AuNMs Protected by Different Types of Ligands Using SEC. The earlier sections covered various aspects of SEC using separation of aliphatic-like ligand-protected AuNMs.[55] Another example with separation of phenylethanethiolate-protected Au_{38} and Au_{144} monitored by MALDI-MS is shown in Figure S4. Nanomolecules with other ligands can also be separated using SEC as it is mostly based on the hydrodynamic volume (size) and there are minimal chemical interactions between the beads and the analyte.[34] In this section, separation of different AuNM sizes protected by thiophenolate, TBBT, and *t*-butyl thiolate ligands is demonstrated.

Thiophenolate-Protected Au_{36}. $Au_{36}(SPh)_{24}$ (refs 51 and 52) can be separated using the same SEC separation protocol. Figure 4 shows the MALDI mass spectra of different fractions collected from an SEC column for separation of $Au_{36}(SPh)_{24}$ from other larger and smaller sizes. The peak observed at ∼8400 m/z units in the mass spectra corresponds to a fragment of $Au_{36}(SPh)_{24}$. The etched product appeared to be pure with no peaks at a higher mass range. However, upon SEC, the first three fractions showed MALDI peaks for larger nanomolecules that are obscured in the mass spectrum of the etched product due to the relatively high peak intensities of lower sizes. SEC can be used to readily eliminate such minor amounts of impurities to obtain monodisperse samples. Fractions F8 and F9 had highly pure $Au_{36}(SPh)_{24}$.

Phenylethanethiolate-Protected Au_{144} and Au_{38}. $Au_{144}(SR)_{60}$ is one of the most stable AuNMs and has been of broad interest.[3,17,56−62] Au_{144} was observed in etching reactions and can be separated from a mixture of different sizes using SEC. A mixture of Au_{144}, Au_{329}, and other smaller species

https://dx.doi.org/10.1021/acs.analchem.0c04961
Anal. Chem. 2021, 93, 3987−3996

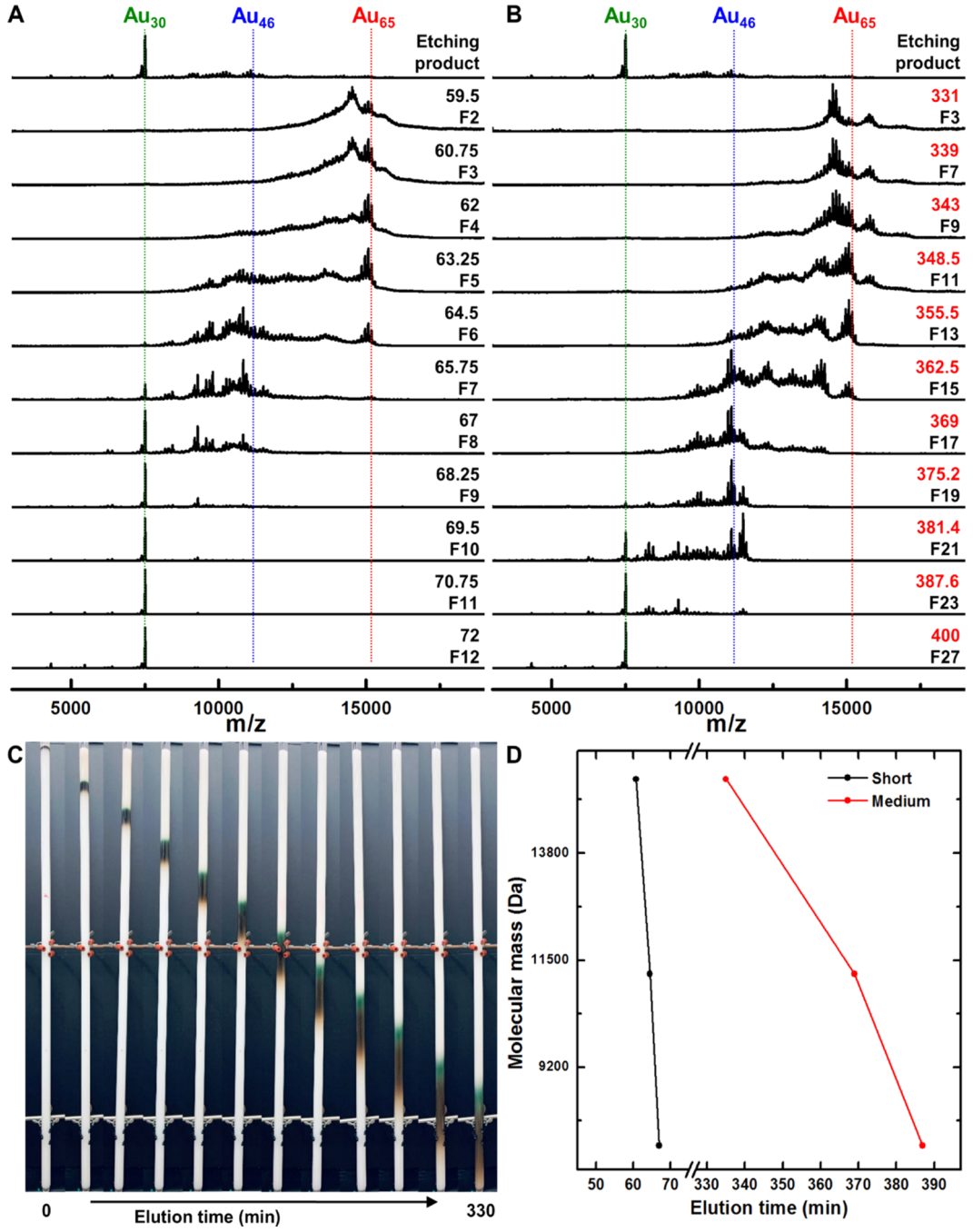

Figure 6. SEC of *t*-butyl thiolate-protected AuNM etched product containing $Au_{30}(SR)_{18}$ (7514 Da), $Au_{46}(SR)_{24}$ (11200 Da), and $Au_{65}(SR)_{29}$ (15389 Da). MALDI-MS showing different fractions collected during SEC using (A) short and (B) medium columns with elution time in minutes and fraction numbers. (C) Pictures of the SEC band during elution at a 30 min time interval from loading (0 min) to right before elution (330 min). (D) Molecular weight vs elution time plot reveals the increase in resolution with column length (for separation of Au_{30}, Au_{46}, and Au_{65}).

was used as the starting material. Figure S4 shows the MALDI mass spectra of different fractions collected from the column. Fraction F3 showed peaks corresponding to Au_{144} and larger sizes. Fraction F4 was pure Au_{144}. F5 and F6 had $Au_{\sim 103-105}$ and Au_{67} nanomolecules. Fractions F7 and F8 have pure Au_{38}. One separation cycle yielded pure Au_{144} and Au_{38}. Such a separation is not attainable by solvent fractionation and demonstrates the advantage of SEC.

TBBT-Protected Au_{28}, Au_{36}, and Au_{44}. In the recent years, crystal structures of several TBBT-protected AuNMs[8−19,63] have been reported. Bulkiness and rigidity of the TBBT ligand[47] favors crystal growth, making it an interesting candidate to be pursued widely. Versatility of SEC in separating closely related sizes, that is, $Au_{28}(SR)_{20}$,[64] $Au_{36}(SR)_{24}$,[65] $Au_{44}(SR)_{28}$,[66] and $Au_{92}(SR)_{44}$[67,68] (8820−25,393 Da) (SR-TBBT) from a polydisperse etched product is demonstrated here (Figure 5). In this separation, pure $Au_{44}(SR)_{28}$ and $Au_{28}(SR)_{20}$ were obtained in F3 and F7, respectively. $Au_{36}(SR)_{24}$ was found as a mixture due to a low number of fractions collected (or a large sample volume collected within the given elution time) in fractions F4 and F5. Fractions F1 and F2 had a mixture of smaller sizes along with

https://dx.doi.org/10.1021/acs.analchem.0c04961
Anal. Chem. 2021, 93, 3987−3996

$Au_{92}(SR)_{44}$. The three nanomolecules [$Au_{44}(SR)_{28}$, $Au_{36}(SR)_{24}$, and $Au_{28}(SR)_{20}$] having a size difference of ∼0.1 nm have been separated in one cycle, indicating that the isolation of nanomolecules in a close size range can be achieved effectively using SEC, independent of the type of the protecting ligand.

Separation of *t*-Butyl Thiolate-Protected AuNMs and the Effect of Column Length on Resolution. We have used a mixture of Au_{30}(S-*t*Bu)$_{18}$ (7514 Da), Au_{46}(S-*t*Bu)$_{24}$ (11,200 Da), and Au_{65}(S-*t*Bu)$_{29}$ (15,389 Da) as the starting material (hereinafter denoted as Au_{30}, Au_{46}, and Au_{65}, respectively) to illustrate the separation of AuNMs protected by the bulky ligand using SEC and that the resolution increases with column length. SEC was performed using short (Figure 6A) and medium (Figure 6B) columns. The separation of each species as it elutes through the column can be identified visually as well (Figure 6C). The leftmost picture was taken immediately after loading the sample as a thin loaded layer. The band expands and the AuNMs separate as they elute through the column. The rightmost image was taken before collecting the fractions and shows the maximum expanded band (the short column images are shown in Figure S5). The green band at the top was followed by the dark-brown band at the middle, and the light-brown band was at the bottom. The first fraction was collected 57 min after loading the sample. In total, 12 fractions were collected for the short column. Each fraction was collected for 75 s and named F1, F2, etc.

The elution time for the medium column increased to ∼5.5 h, that is, 5.5 times more than that for the short column (∼1 h). The length of the medium column is ∼2.5 times longer than the short column. The medium column yielded a more expanded band during elution, resulting in a better separation compared to the short column. The band expands slowly in the 1.5−2 h of elution (Figure 6C). Then, it expands well toward 3 h and continues to expand till elution. In the medium column, it took 330 min to elute the first fraction. It separated two bands with minimum mixing, whereas the short column has more mixing of bands. A total of 27 fractions were collected. Each fraction in F1−F10, F11−F15, and F16−F27 was collected for 120, 210, and 190 s, respectively.

The fractions collected from the short and medium columns were analyzed by MALDI-MS (Figure 6A,B, a few similar fractions were excluded for clarity). The etched product has Au_{30} as a major peak, and Au_{46} and Au_{65} peaks were minor. In the short column fractions, F2−F4 have Au_{65}, F5 and F6 have both Au_{65} and Au_{46}, F7 and F8 have both Au_{46} and Au_{30}, and F9−F12 have Au_{30}. A fraction with major or pure Au_{46} was not obtained in the short column. The short column SEC peak widths for Au_{65}, Au_{46}, and Au_{30} were 7.5, 3.75, and 7.5 min, respectively. In the medium column, F5−F11 have Au_{65}, F13−F15 have Au_{65} and Au_{46}, F17−F19 have Au_{46}, F21−F23 have Au_{46} and Au_{30}, and F25−F27 have pure Au_{30}. The medium column SEC peak widths for Au_{65}, Au_{46}, and Au_{30} were 38.8, 39.1, and 21.7 min, respectively. The elution time for the first fraction going from the short column to the medium column increased from 57 to 330 min. Unlike the short column, we were able to get fractions containing Au_{46} as a major species using the medium column. The increase in length of the column improves the resolution, and it can be readily seen in Figure 6D, where the entire elution window from the first fraction to the last is 12 min for the short column, whereas it is 70 min for the medium column. The green-colored Au_{30} NM elutes last and could be visually distinguished to be collected as a pure fraction. Pure Au_{46} and Au_{65} could also be obtained by repetition of a few SEC cycles using fractions having the same size distribution.

CONCLUSIONS

In summary, several sizes of AuNMs can be isolated effectively using the gravity flow SEC technique in a semi-preparative or preparative scale with much better control. The size range for separation of AuNMs using SEC has been illustrated to work up to ∼200 kDa, making this technique suitable for isolation of a majority of nanomolecule sizes reported to date. The versatility of SEC was also demonstrated with several examples. The separation of different sizes of nanomolecules protected with different types of ligands proves that SEC can be used for isolation of highly monodisperse nanomolecules irrespective of the types of ligands. Monodispersity (purity) can further be improved by performing multiple cycles of SEC. Separation of closely related sizes is challenging, but it is achievable through multiple cycles of SEC as demonstrated through the separation of $Au_{137}(SR)_{56}$ from a mixture of $Au_{329}(SR)_{84}$, $Au_{144}(SR)_{60}$, $Au_{137}(SR)_{56}$, and $Au_{130}(SR)_{50}$. The same protocol can be applied for isolation of any nanomolecule observed in a mixture. However, if the nanomolecule was present in very minor amounts, isolation could become increasingly difficult. By far, gravity flow SEC appears to be the efficient technique for the separation of organosoluble AuNMs with ease of use, and it would greatly contribute to the progress of the field.

ASSOCIATED CONTENT

Supporting Information

The Supporting Information is available free of charge at https://pubs.acs.org/doi/10.1021/acs.analchem.0c04961.

Supporting mass spectra and additional data (PDF)

AUTHOR INFORMATION

Corresponding Author

Amala Dass − *Department of Chemistry and Biochemistry, University of Mississippi, Oxford, Mississippi 38677, United States;* orcid.org/0000-0001-6942-5451; Email: amal@olemiss.edu

Authors

Naga Arjun Sakthivel − *Department of Chemistry and Biochemistry, University of Mississippi, Oxford, Mississippi 38677, United States;* orcid.org/0000-0001-8134-905X

Vijay Reddy Jupally − *Department of Chemistry and Biochemistry, University of Mississippi, Oxford, Mississippi 38677, United States*

Senthil Kumar Eswaramoorthy − *Department of Chemistry and Biochemistry, University of Mississippi, Oxford, Mississippi 38677, United States;* orcid.org/0000-0001-8015-1391

Kalpani Hirunika Wijesinghe − *Department of Chemistry and Biochemistry, University of Mississippi, Oxford, Mississippi 38677, United States;* orcid.org/0000-0002-7049-0370

Praneeth Reddy Nimmala − *Department of Chemistry and Biochemistry, University of Mississippi, Oxford, Mississippi 38677, United States*

Chanaka Kumara − *Department of Chemistry and Biochemistry, University of Mississippi, Oxford, Mississippi 38677, United States;* orcid.org/0000-0002-1496-8886

https://dx.doi.org/10.1021/acs.analchem.0c04961
Anal. Chem. 2021, 93, 3987−3996

Milan Rambukwella − *Department of Chemistry and Biochemistry, University of Mississippi, Oxford, Mississippi 38677, United States*

Tanya Jones − *Department of Chemistry and Biochemistry, University of Mississippi, Oxford, Mississippi 38677, United States*

Complete contact information is available at: https://pubs.acs.org/10.1021/acs.analchem.0c04961

Author Contributions

†N.A.S. and V.R.J. contributed equally.

Notes

The authors declare no competing financial interest.

■ ACKNOWLEDGMENTS

NSF-CHE-1808138 and NSF-CHE-1255519 supported this work. The authors gratefully acknowledge the support from Vigneshraja Ganeshraj.

■ REFERENCES

(1) Whetten, R. L.; Khoury, J. T.; Alvarez, M. M.; Murthy, S.; Vezmar, I.; Wang, Z. L.; Stephens, P. W.; Cleveland, C. L.; Luedtke, W. D.; Landman, U. *Adv. Mater.* **1996**, *8*, 428−433.
(2) Hostetler, M. J.; Green, S. J.; Stokes, J. J.; Murray, R. W. *J. Am. Chem. Soc.* **1996**, *118*, 4212−4213.
(3) Chen, S.; Ingram, R. S.; Hostetler, M. J.; Pietron, J. J.; Murray, R. W.; Schaaff, T. G.; Khoury, J. T.; Alvarez, M. M.; Whetten, R. L. *Science* **1998**, *280*, 2098−2101.
(4) Heaven, M. W.; Dass, A.; White, P. S.; Holt, K. M.; Murray, R. W. *J. Am. Chem. Soc.* **2008**, *130*, 3754−3755.
(5) Jadzinsky, P. D.; Calero, G.; Ackerson, C. J.; Bushnell, D. A.; Kornberg, R. D. *Science* **2007**, *318*, 430−433.
(6) Brust, M.; Walker, M.; Bethell, D.; Schiffrin, D. J.; Whyman, R. *J. Chem. Soc., Chem. Commun.* **1994**, 801−802.
(7) Schaaff, T. G.; Whetten, R. L. *J. Phys. Chem. B* **1999**, *103*, 9394−9396.
(8) Dass, A. *J. Am. Chem. Soc.* **2011**, *133*, 19259−19261.
(9) Sakthivel, N. A.; Shabaninezhad, M.; Sementa, L.; Yoon, B.; Stener, M.; Whetten, R. L.; Ramakrishna, G.; Fortunelli, A.; Landman, U.; Dass, A. *J. Am. Chem. Soc.* **2020**, *142*, 15799−15814.
(10) Alvarez, M. M.; Khoury, J. T.; Schaaff, T. G.; Shafigullin, M. N.; Vezmar, I.; Whetten, R. L. *J. Phys. Chem. B* **1997**, *101*, 3706−3712.
(11) Kwak, K.; Thanthirige, V. D.; Pyo, K.; Lee, D.; Ramakrishna, G. *J. Phys. Chem. Lett.* **2017**, *8*, 4898−4905.
(12) Hartland, G. V. *Chem. Rev.* **2011**, *111*, 3858−3887.
(13) Fernando, A.; Weerawardene, K. L. D. M.; Karimova, N. V.; Aikens, C. M. *Chem. Rev.* **2015**, *115*, 6112−6216.
(14) Walter, M.; Akola, J.; Lopez-Acevedo, O.; Jadzinsky, P. D.; Calero, G.; Ackerson, C. J.; Whetten, R. L.; Grönbeck, H.; Häkkinen, H. *Proc. Natl. Acad. Sci. U.S.A.* **2008**, *105*, 9157−9162.
(15) Link, S.; El-Sayed, M. A.; Gregory Schaaff, T.; Whetten, R. L. *Chem. Phys. Lett.* **2002**, *356*, 240−246.
(16) Cleveland, C. L.; Landman, U.; Shafigullin, M. N.; Stephens, P. W.; Whetten, R. L. *Z. Phys. D* **1997**, *40*, 503−508.
(17) Schaaff, T. G.; Shafigullin, M. N.; Khoury, J. T.; Vezmar, I.; Whetten, R. L. *J. Phys. Chem. B* **2001**, *105*, 8785−8796.
(18) Schaaff, T. G.; Shafigullin, M. N.; Khoury, J. T.; Vezmar, I.; Whetten, R. L.; Cullen, W. G.; First, P. N.; Gutiérrez-Wing, C.; Ascensio, J.; Jose-Yacamán, M. J. *J. Phys. Chem. B* **1997**, *101*, 7885−7891.
(19) Price, R. C.; Whetten, R. L. *J. Am. Chem. Soc.* **2005**, *127*, 13750−13751.
(20) Daniel, M.-C.; Astruc, D. *Chem. Rev.* **2004**, *104*, 293−346.
(21) Du, Y.; Sheng, H.; Astruc, D.; Zhu, M. *Chem. Rev.* **2020**, *120*, 526−622.
(22) Liu, H.; Hong, G.; Luo, Z.; Chen, J.; Chang, J.; Gong, M.; He, H.; Yang, J.; Yuan, X.; Li, L.; Mu, X.; Wang, J.; Mi, W.; Luo, J.; Xie, J.; Zhang, X. D. *Adv. Mater.* **2019**, *31*, 1901015.
(23) Nimmala, P. R.; Yoon, B.; Whetten, R. L.; Landman, U.; Dass, A. *J. Phys. Chem. A* **2013**, *117*, 504−517.
(24) Jimenez, V. L.; Leopold, M. C.; Mazzitelli, C.; Jorgenson, J. W.; Murray, R. W. *Anal. Chem.* **2003**, *75*, 199−206.
(25) Negishi, Y.; Sakamoto, C.; Ohyama, T.; Tsukuda, T. *J. Phys. Chem. Lett.* **2012**, *3*, 1624−1628.
(26) Negishi, Y.; Nakazaki, T.; Malola, S.; Takano, S.; Niihori, Y.; Kurashige, W.; Yamazoe, S.; Tsukuda, T.; Häkkinen, H. *J. Am. Chem. Soc.* **2015**, *137*, 1206−1212.
(27) Black, D. M.; Robles, G.; Bach, S. B. H.; Whetten, R. L. *Ind. Eng. Chem. Res.* **2018**, *57*, 5378−5384.
(28) Knoppe, S.; Vogt, P. *Anal. Chem.* **2019**, *91*, 1603−1609.
(29) Black, D. M.; Bhattarai, N.; Bach, S. B. H.; Whetten, R. L. *J. Phys. Chem. Lett.* **2016**, *7*, 3199−3205.
(30) Sugi, K. S.; Bhat, S.; Nag, A.; Ganesan, P.; Mahendranath, A.; Pradeep, T. *Analyst* **2020**, *145*, 1337−1345.
(31) Wilcoxon, J. P.; Martin, J. E.; Provencio, P. *Langmuir* **2000**, *16*, 9912−9920.
(32) Wilcoxon, J. P.; Provencio, P. *J. Phys. Chem. B* **2003**, *107*, 12949−12957.
(33) Tsunoyama, H.; Negishi, Y.; Tsukuda, T. *J. Am. Chem. Soc.* **2006**, *128*, 6036−6037.
(34) Knoppe, S.; Boudon, J.; Dolamic, I.; Dass, A.; Bürgi, T. *Anal. Chem.* **2011**, *83*, 5056−5061.
(35) Qian, H.; Zhu, Y.; Jin, R. *J. Am. Chem. Soc.* **2010**, *132*, 4583−4585.
(36) Jupally, V. R.; Dharmaratne, A. C.; Crasto, D.; Huckaba, A. J.; Kumara, C.; Nimmala, P. R.; Kothalawala, N.; Delcamp, J. H.; Dass, A. *Chem. Commun.* **2014**, *50*, 9895−9898.
(37) Tian, S.; Li, Y.-Z.; Li, M.-B.; Yuan, J.; Yang, J.; Wu, Z.; Jin, R. *Nat. Commun.* **2015**, *6*, 8667.
(38) Dainese, T.; Antonello, S.; Gascón, J. A.; Pan, F.; Perera, N. V.; Ruzzi, M.; Venzo, A.; Zoleo, A.; Rissanen, K.; Maran, F. *ACS Nano* **2014**, *8*, 3904−3912.
(39) Gautier, C.; Bürgi, T. *J. Am. Chem. Soc.* **2006**, *128*, 11079−11087.
(40) Desireddy, A.; Conn, B. E.; Guo, J.; Yoon, B.; Barnett, R. N.; Monahan, B. M.; Kirschbaum, K.; Griffith, W. P.; Whetten, R. L.; Landman, U.; Bigioni, T. P. *Nature* **2013**, *501*, 399−402.
(41) Negishi, Y.; Hashimoto, S.; Ebina, A.; Hamada, K.; Hossain, S.; Kawawaki, T. *Nanoscale* **2020**, *12*, 8017−8039.
(42) Black, D. M.; Robles, G.; Lopez, P.; Bach, S. B. H.; Alvarez, M.; Whetten, R. L. *Anal. Chem.* **2018**, *90*, 2010−2017.
(43) Barth, H. G.; Boyes, B. E.; Jackson, C. *Anal. Chem.* **1996**, *68*, 445−466.
(44) Barth, H. G.; Boyes, B. E.; Jackson, C. *Anal. Chem.* **1998**, *70*, 251−278.
(45) Bio-Beads S-X Resin. Biorad laboratories http://www.biorad.com/webroot/web/pdf/lsr/literature/LIT263.pdf (accessed February 17, 2021).
(46) Dass, A.; Sakthivel, N. A.; Jupally, V. R.; Kumara, C.; Rambukwella, M. *ACS Energy Lett.* **2020**, *5*, 207−214.
(47) Dass, A.; Theivendran, S.; Nimmala, P. R.; Kumara, C.; Jupally, V. R.; Fortunelli, A.; Sementa, L.; Barcaro, G.; Zuo, X.; Noll, B. C. *J. Am. Chem. Soc.* **2015**, *137*, 4610−4613.
(48) Sakthivel, N. A.; Theivendran, S.; Ganeshraj, V.; Oliver, A. G.; Dass, A. *J. Am. Chem. Soc.* **2017**, *139*, 15450−15459.
(49) Jones, T. C.; Sumner, L.; Ramakrishna, G.; Hatshan, M. b.; Abuhagr, A.; Chakraborty, S.; Dass, A. *J. Phys. Chem. C* **2018**, *122*, 17726−17737.
(50) Dass, A.; Nimmala, P. R.; Jupally, V. R.; Kothalawala, N. *Nanoscale* **2013**, *5*, 12082−12085.
(51) Nimmala, P. R.; Dass, A. *J. Am. Chem. Soc.* **2011**, *133*, 9175−9177.
(52) Nimmala, P. R.; Knoppe, S.; Jupally, V. R.; Delcamp, J. H.; Aikens, C. M.; Dass, A. *J. Phys. Chem. B* **2014**, *118*, 14157−14167.

(53) Sakthivel, N. A.; Stener, M.; Sementa, L.; Fortunelli, A.; Ramakrishna, G.; Dass, A. *J. Phys. Chem. Lett.* **2018**, *9*, 1295−1300.
(54) Dharmaratne, A. C.; Krick, T.; Dass, A. *J. Am. Chem. Soc.* **2009**, *131*, 13604−13605.
(55) Jupally, V. R.; Dass, A. *Phys. Chem. Chem. Phys.* **2014**, *16*, 10473−10479.
(56) Chaki, N. K.; Negishi, Y.; Tsunoyama, H.; Shichibu, Y.; Tsukuda, T. *J. Am. Chem. Soc.* **2008**, *130*, 8608−8610.
(57) Yan, N.; Xia, N.; Liao, L.; Zhu, M.; Jin, F.; Jin, R.; Wu, Z. *Sci. Adv.* **2018**, *4*, No. eaat7259.
(58) Lopez-Acevedo, O.; Akola, J.; Whetten, R. L.; Grönbeck, H.; Häkkinen, H. *J. Phys. Chem. C* **2009**, *113*, 5035−5038.
(59) Lei, Z.; Li, J.-J.; Wan, X.-K.; Zhang, W.-H.; Wang, Q.-M. *Angew. Chem. Int. Ed.* **2018**, *57*, 8639−8643.
(60) Jensen, K. M. Ø.; Juhas, P.; Tofanelli, M. A.; Heinecke, C. L.; Vaughan, G.; Ackerson, C. J.; Billinge, S. J. L. *Nat. Commun.* **2016**, *7*, 11859.
(61) Yi, C.; Tofanelli, M. A.; Ackerson, C. J.; Knappenberger, K. L. *J. Am. Chem. Soc.* **2013**, *135*, 18222−18228.
(62) Quinn, B. M.; Liljeroth, P.; Ruiz, V.; Laaksonen, T.; Kontturi, K. *J. Am. Chem. Soc.* **2003**, *125*, 6644−6645.
(63) Sakthivel, N. A.; Dass, A. *Acc. Chem. Res.* **2018**, *51*, 1774−1783.
(64) Zeng, C.; Li, T.; Das, A.; Rosi, N. L.; Jin, R. *J. Am. Chem. Soc.* **2013**, *135*, 10011−10013.
(65) Zeng, C.; Qian, H.; Li, T.; Li, G.; Rosi, N. L.; Yoon, B.; Barnett, R. N.; Whetten, R. L.; Landman, U.; Jin, R. *Angew. Chem., Int. Ed.* **2012**, *51*, 13114−13118.
(66) Zeng, C.; Chen, Y.; Iida, K.; Nobusada, K.; Kirschbaum, K.; Lambright, K. J.; Jin, R. *J. Am. Chem. Soc.* **2016**, *138*, 3950−3953.
(67) Zeng, C.; Liu, C.; Chen, Y.; Rosi, N. L.; Jin, R. *J. Am. Chem. Soc.* **2016**, *138*, 8710−8713.
(68) Liao, L.; Chen, J.; Wang, C.; Zhuang, S.; Yan, N.; Yao, C.; Xia, N.; Li, L.; Bao, X.; Wu, Z. *Chem. Commun.* **2016**, *52*, 12036−12039.

https://dx.doi.org/10.1021/acs.analchem.0c04961
Anal. Chem. 2021, 93, 3987−3996